

Compositional dependence of longitudinal sound velocities of piezoelectric (111) $\text{In}_x\text{Ga}_{(1-x)}\text{As}$ measured by picosecond ultrasonics

Yu-Chieh Wen

*Department of Electrical Engineering, National Taiwan University, Taipei 10617, Taiwan
and Graduate Institute of Electro-Optical Engineering, National Taiwan University, Taipei 10617, Taiwan*

Li-Chang Chou and Hao-Hsiung Lin

*Department of Electrical Engineering, National Taiwan University, Taipei 10617, Taiwan
and Graduate Institute of Electronics Engineering, National Taiwan University, Taipei 10617, Taiwan*

Kung-Hsuan Lin, Tzeng-Fu Kao, and Chi-Kuang Sun^{a)}

*Department of Electrical Engineering, National Taiwan University, Taipei 10617, Taiwan
and Graduate Institute of Electro-Optical Engineering, National Taiwan University, Taipei 10617, Taiwan*

(Received 14 March 2006; accepted 8 September 2006; published online 21 November 2006)

Picosecond ultrasonic experiments were performed to generate and detect acoustic pulses in piezoelectric (111) epilayers of $\text{In}_x\text{Ga}_{(1-x)}\text{As}$, and the longitudinal sound velocities in the [111] direction of $\text{In}_x\text{Ga}_{(1-x)}\text{As}$ were thus directly determined by controlling the indium content x . We found that the sound velocity exhibits an obvious bowing with different alloy compositions and can be described as a quadratic function of $V_L(x) = 458x^2 - 1451x + 5414$. This result supports a nonlinear compositional dependence of the elastic constants of $\text{In}_x\text{Ga}_{(1-x)}\text{As}$ and indicates that the linear-interpolation approximation is inapplicable for estimating sound velocity in this specific case. © 2006 American Institute of Physics. [DOI: 10.1063/1.2388138]

I. INTRODUCTION

Piezoelectric semiconductors have recently attracted much interest due to its characteristics of acousto-optical and electroacoustic couplings.¹⁻⁴ One of these piezoelectric semiconductors is strained (111)-oriented InGaAs, which can be grown in high quality as heterostructures with high built-in piezoelectric fields.⁵ Therefore it is highly desired to explore its potential for future GaAs-based acousto-optical devices. However, the lack of study on the elastic properties of the InAs-GaAs system makes it difficult to precisely design acousto-optical devices from those compounds.

With a zinc blende cubic structure in InGaAs, strong coupling between the piezoelectric field and the ultrasonic wave propagation along the [111] direction can be expected and one can anticipate that the mode of acoustic waves propagating along the [111] direction would play an important role in piezoelectric device applications. The longitudinal sound velocity along the [111] direction is one of the most significant elastic properties to be determined. For most binary compounds such as InAs and GaAs, one can calculate sound velocities from its elastic constants by the well-known elastic relations (e.g., Christoffel's equation).⁶ As for $\text{In}_x\text{Ga}_{(1-x)}\text{As}$, not only its sound velocities but also its elastic constants are still unattainable. Therefore, they are usually estimated by a linear-interpolation approximation from the elastic properties of InAs and GaAs.⁷ When using linear-interpolation method to investigate sound velocities of ternary compounds, there are two different assumptions generally adopted. One is linear dependence of sound velocity

with composition parameter x .⁷ The other is to consider a linear relation between the elastic constants and the alloy content.⁸ Although these linear-interpolation methods are widely used for the sound velocity estimation, many previous studies show that the elastic constants of III-V ternary compounds exhibit bowing with the alloy composition.⁹⁻¹¹ It is thus highly desirable to experimentally determine the alloy composition dependence of the longitudinal sound velocity along the [111] direction in InGaAs.

In this paper, we performed picosecond ultrasonic experiments to study the elastic properties of $\text{In}_x\text{Ga}_{(1-x)}\text{As}$ with different alloy compositions. By directly generating and observing the acoustic pulses propagating along the [111] direction, we experimentally determined the longitudinal sound velocity along the [111] direction as a function of indium content x . These results showed an obvious bowing relation between the sound velocity and the indium composition and indicated a nonlinearly compositional dependence of the elastic constants of $\text{In}_x\text{Ga}_{(1-x)}\text{As}$. Moreover, our study revealed that the linear-interpolation approximation is unsuitable for estimating the sound velocity along the [111] direction of $\text{In}_x\text{Ga}_{(1-x)}\text{As}$.

II. PICOSECOND ULTRASONICS AND EXPERIMENTAL SETUP

A. Picosecond ultrasonics

With the advances of ultrafast laser technologies, the so-called "picosecond ultrasonics" is developed to generate picosecond acoustic pulses with a central frequency up to several hundred gigahertz and to study the acoustic and thermal properties of thin films.¹²⁻¹⁵ Figure 1 shows the schematic diagram of the adopted picosecond ultrasonic measurement

^{a)}Author to whom correspondence should be addressed; electronic mail: sun@cc.ee.ntu.edu.tw

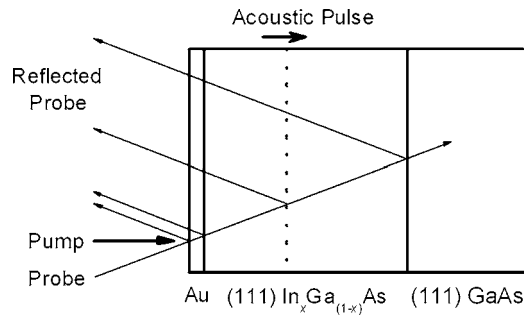


FIG. 1. Schematic diagram of the picosecond ultrasonic experiment. The acoustic pulse was excited by an optical pump pulse and was monitored by the interference behavior of a reflected probe pulse between the interfaces of the sample and the region where refractive index was modulated by the acoustic pulse.

in this study. First a femtosecond optical IR pulse (referred to as the “pump pulse”) was incident onto a 10-nm-thick gold film sputtered on the surface of the InGaAs sample and was used to generate the acoustic pulses. After the optical pulse was strongly absorbed by the gold film, a sudden increase in the film temperature of a few degrees Kelvin would be induced.¹³ This temperature rise generated a thermal stress distribution in the gold film that initiated a strain pulse into the InGaAs layer. The initiated acoustic pulsewidth is determined by the gold film thickness and the sound velocity of the gold film. Because the film thickness was much smaller than the laser spot size (typically a few tens of microns in diameter), only the longitudinal acoustic waves were excited. The photoexcited acoustic pulses then propagated into the studied InGaAs layer with the longitudinal sound velocity and were monitored by another time-delayed optical pulse (referred as the “probe pulse”). With the refractive index modified by the strain field, the transmission or reflection changes of the optical probe pulse can be used to study sound velocities, attenuation of traveling acoustic waves, and thicknesses of thin films.^{12–14} In our specific case, we utilized the time-resolved “Brillouin scatterings” of the probe beam to measure the longitudinal sound velocity.^{12,15} The reflected probe beams from the “fixed” interfaces of the sample (for example, the top surface) interfered with that from the “dynamic” region where refractive index was altered by the propagating acoustic pulses. With the propagation of acoustic pulses, the phase relation between the reflected optical beams changed with time, which resulted in the transient oscillatory reflection of the probe pulse. This oscillation frequency can be derived as¹⁴

$$f = \frac{2nV \cos \theta}{\lambda}, \quad (1)$$

where n and V are the refractive index and the longitudinal sound velocity of the propagation layer, λ is the vacuum wavelength of the light, and θ is the angle between the propagation directions of the optical probe pulse and the acoustic pulses. From Eq. (1), the longitudinal sound velocity can then be obtained by measuring the oscillation frequency.

B. Experimental details

For most applications of (111) InGaAs heterostructures with built-in strain-induced piezoelectric fields, the indium concentration is hardly higher than 35% to avoid strain relaxation in the InGaAs layers.¹⁶ One of the aims of the present study is to determine sound velocities for applications of acousto-optical devices. We therefore reduced the measured regime of In composition by choosing $0 \leq x \leq 0.3$. Moreover, with the previous investigation of sound velocities in InAs the observed regime of In content could be extended, and the relation between the In content x and the longitudinal sound velocity along the [111] direction, $V_L[111]$, of $\text{In}_x\text{Ga}_{(1-x)}\text{As}$ can thus be established.

The samples under study were (111) $\text{In}_x\text{Ga}_{(1-x)}\text{As}$ thin films with indium compositions $x=0, 0.1, 0.2, 0.3$. The indium content of each sample was measured by using electron probe x-ray microanalyzer (EPMA). $\text{In}_x\text{Ga}_{(1-x)}\text{As}$ layers with $\sim 1.5 \mu\text{m}$ thickness were grown on (111) GaAs substrates by the molecular-beam epitaxy (MBE) technique. In addition, the surfaces of the samples were sputtered with a 10-nm-thick gold thin film as the generation layer for initiating acoustic pulses. With an $\text{In}_x\text{Ga}_{(1-x)}\text{As}$ layer thickness much greater than the critical thickness,¹⁷ the strain due to the lattice mismatch can be expected to be fully relaxed. The typical dislocation density in InGaAs/GaAs heterostructures, depending on the growth conditions and film thickness, is on the order of 10^7 cm^{-2} .¹⁸ According to a previous elastic study in GaN films with different dislocation densities,¹⁹ the discrepancy in the sound velocity due to dislocation is insignificant in contrast to our measurement uncertainty even with a dislocation density up to $10^8\text{--}10^{10} \text{ cm}^{-2}$. We thus assumed that the dislocation-induced sound velocity deviation in our samples could be on the order of or below our system resolution.

It is clear from Eq. (1) that the reduction of estimation error in the refractive index is essential to improve the accuracy of the sound velocity measurements. For semiconductor materials, the refractive index will vary abruptly when the optical wavelength approaches to the bandgap, which is strongly dependent on the sample quality.²⁰ In addition, with the probe photon energy above the bandgap energy, strong absorption would result in low probe penetration. The probe wavelength adopted in this measurement was thus chosen to be $1.3 \mu\text{m}$, which is much longer than the bandgap wavelengths of all measured samples so that the probe absorption and the uncertainties in refractive indices can be reduced (the bandgap energy of $\text{In}_{0.3}\text{Ga}_{0.7}\text{As}$ is $\sim 1.05 \text{ eV}$, corresponding to an optical wavelength of $1.18 \mu\text{m}$, at room temperature²¹). The $1.3 \mu\text{m}$ wavelength can be reached by using an optical parametric oscillator (OPO) synchronously pumped by a mode-locked Ti:sapphire laser. With collinear noncritically phase-matched parametric interaction in a periodically poled lithium niobate (PPLN) crystal, the OPO was able to convert the near-infrared beam into infrared with a pulse width on the order of 200 fs at a repetition rate of 76 MHz. The corresponding coherence time for the acoustic-pulse-induced

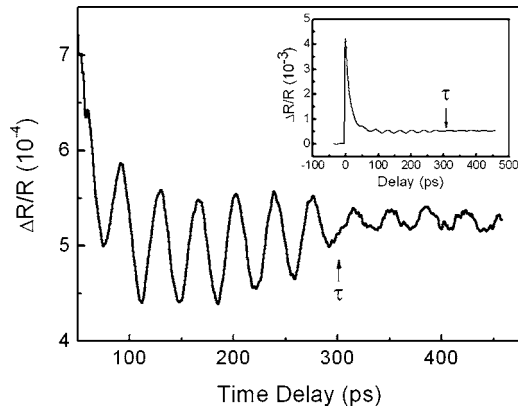


FIG. 2. The measured optical reflection change as a function of time delay for the sample of $\text{In}_{0.3}\text{Ga}_{0.7}\text{As}$. τ is the time at which the acoustic pulse entered the (111) GaAs substrate. The oscillations at the frequencies of 27.0 and 28.3 GHz resulted from the propagation of the acoustic pulse in InGaAs and GaAs layers were observed. The complete trace is shown in the inset.

optical interference is on the order of 2 ns, which is much longer than the interference delay that occurred in this study.²²

The picosecond ultrasonic experiments were performed using a typical pump-probe arrangement.¹ The laser beam from OPO was split into two beams with perpendicular polarizations. The probe pulse with an average power of 8 mW was delayed with respect to the pump pulse by a mechanical stage. The pump beam at the same wavelength was chopped and was with an average power of 60 mW. Both beams were focused into the sample with a focal diameter of $\sim 15 \mu\text{m}$ and an angle θ of $\sim 5^\circ$. To increase the signal-to-noise ratio, the reflected probe signal was measured using a lock-in amplifier as a function of the temporal delay between the pump and the probe pulses.

III. RESULTS AND DISCUSSION

A. Experimental results

Figure 2 shows a typically measured probe reflection change as a function of time delay for the sample with $x = 0.3$. When the Au film was heated by the pump pulse, the temperature rise induced the reflectivity change by the thermoreflectance effect. The reflectivity change then slowly disappeared as the heat diffused into the sample. With an average pump power of 60 mW, an oscillation signal with a modulation strength $\Delta R/R$ on the order of 10^{-4} could be observed on top of the background signal. This oscillation signal resulted from the Brillouin scattering effect as described in previous discussions. Before ~ 300 ps, the observed oscillation period of 37 ps, corresponding to a frequency of 27.0 GHz, is attributed to the propagation of longitudinal acoustic pulses in the InGaAs layer. A sudden change of modulation strength could be found at ~ 300 ps, which indicates that the acoustic pulses transmitted into the GaAs substrate after traveling in the InGaAs layer. Because of the small difference between the acoustic impedances of GaAs and InGaAs with a low In content, low reflection of acoustic pulses is expected at the InGaAs/GaAs interface.

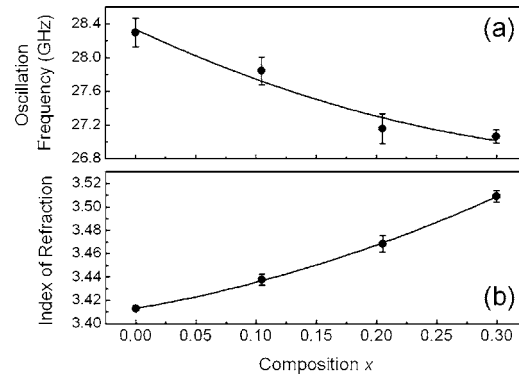


FIG. 3. (a) The measured oscillation frequencies of the optical reflection changes and (b) the calculated indices of refraction for the $\text{In}_x\text{Ga}_{(1-x)}\text{As}$ samples with different In contents.

The change of modulation strength is thus attributed to different sensitivity functions of InGaAs and GaAs.²³

In addition, the compositional dependent refractive index for a wavelength below the bandgap has previously been reported by Takagi.²⁴ From his reported results the refractive index of $\text{In}_{0.3}\text{Ga}_{0.7}\text{As}$ can be estimated as 3.509. The sound velocity of $\text{In}_{0.3}\text{Ga}_{0.7}\text{As}$ along [111], therefore, could be derived as 5033 m/s by using Eq. (1).

B. Result analysis and discussion

In addition to $\text{In}_{0.3}\text{Ga}_{0.7}\text{As}$, the same experiment and calculation for samples of different indium compositions were carried out as shown in Fig. 3. The refractive index becomes higher when the alloy consists of a higher indium concentration. In addition, high indium concentration results in the decrease of the measured oscillation frequency. These results conform to the characteristic that the sound velocity of $\text{In}_x\text{Ga}_{(1-x)}\text{As}$ becomes lower with the increase in the indium content x . The error bars shown in Fig. 3 represent the standard deviation. The error bars on the oscillation frequencies are the statistic results from the measurements performed at different positions on each sample. Those uncertainties are also caused by the limits of signal-to-noise ratio and the analytic uncertainty resulted from finite oscillation periods. Due to the uncertainties of alloy concentration of the measured samples, the variations of calculated refractive indices were taken into consideration and are also shown as the standard deviation in Fig. 3.

According to the measured data and the calculated refractive indices, the compositional dependence of the longitudinal sound velocities of InGaAs along the [111] direction can be obtained. In (111) GaAs the measured values yield $V_L[111] = 5410 \pm 32$ m/s, which is in good agreement with the values obtained from the literature values of the elastic constants,^{6,25,26} as shown in Table I. Figure 4 shows the measured and the expected sound velocities calculated by the reported elastic constants of $\text{In}_x\text{Ga}_{(1-x)}\text{As}$ as a function of the indium composition. The sound velocities determined by our measurements were denoted as solid dots, and the calculated sound velocity of InAs was labeled as solid triangle.^{26,27}

To appropriately model the relation between the longitudinal sound velocity and the indium content x , we first com-

TABLE I. Longitudinal sound velocities of $\text{In}_x\text{Ga}_{(1-x)}\text{As}$ along the [111] direction for different In compositions. The calculated sound velocities along [111] were derived using the literature values of elastic constants and mass densities according to $V_L = \sqrt{(C_{11} + 2C_{12} + 4C_{44})/3\rho}$.

Composition x	Longitudinal sound velocity along the [111] direction (m/s)	
	Calculated values	Experimental values (this work)
0.000 (GaAs)	5401 ^a 5384±25 ^b 5393 ^{c,d}	5410±32
0.105±0.003		5285±32
0.205±0.005		5110±34
0.300±0.001		5033±15
0.49	4746±29 ^{d,e}	
0.53	4753±29 ^{d,e}	
1.000 (InAs)	4421 ^{c,d}	

^aReference 6.

^bReference 25.

^cThe elastic constants were taken from Ref. 26.

^dThe mass densities of $\text{In}_x\text{Ga}_{(1-x)}\text{As}$ were obtained by applying Vegard's rule $\rho = 5317 + 350x$ (kg/cm^3), which was the interpolation of those of GaAs and InAs (Refs. 25 and 27).

^eThe elastic constants were taken from Ref. 10.

pared the experimental results with the linear-interpolation values of the sound velocities from those of GaAs and InAs which was shown as a dashed line. It was clear that the measured sound velocities were obviously smaller than the interpolation results. It thus indicated a nonlinear variation in the sound velocity with different indium concentrations, and the linear-interpolation approximation of sound velocity was inapplicable for the sound velocity estimation in this specific material system.

As previously discussed, by assuming linear dependence of the elastic constants on alloy composition, sound velocities could also be evaluated by the elastic relations. It is another linear-approximation method which can be used to model the measured sound velocities in this study, and has

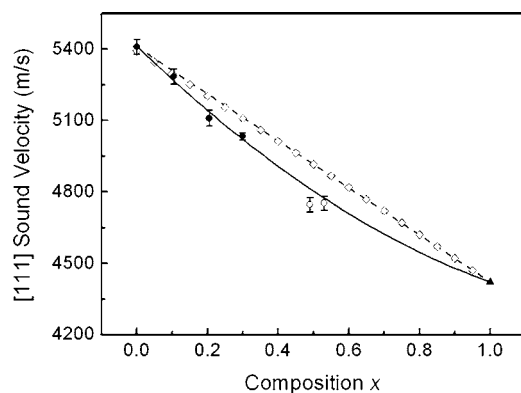


FIG. 4. Longitudinal sound velocity of $\text{In}_x\text{Ga}_{(1-x)}\text{As}$ along the [111] orientation vs the composition x . The measured values are denoted as solid dots, and the calculated ones obtained from the literature values of elastic constants are represented as solid triangles (Ref. 26) and open circles (Ref. 10). The solid line is a quadratic fitting curve according to the measured values of $\text{In}_x\text{Ga}_{(1-x)}\text{As}$ and the calculated sound velocity of InAs. The linear-interpolation curve of the sound velocity is shown in dashed line, and the open rhombuses are the calculated values by assuming linear compositional dependence of elastic constants of $\text{In}_x\text{Ga}_{(1-x)}\text{As}$.

been adopted for the sound velocity investigation in other ternary compounds.⁸ According to Christoffel's equation, the longitudinal sound velocity along the [111] direction of a cubic structure can be formulated as $V_L = \sqrt{(C_{11} + 2C_{12} + 4C_{44})/3\rho}$.⁶ This formula has neglected the stiffening induced by piezoelectric effect because piezoelectric coupling only resulted in $\sim 0.1\%$ and $\sim 0.01\%$ increases in the calculated $V_L[111]$ of GaAs and InAs, respectively.^{6,28} With this elastic relation and the assumption of linear compositional dependence of the elastic constants, the $V_L[111]$ of $\text{In}_x\text{Ga}_{(1-x)}\text{As}$ was calculated and is denoted as open rhombuses in Fig. 4.²⁵⁻²⁷ We could find that the linear estimates of the sound velocity are evidently distinct from the measured values with higher indium contents. It therefore indicates that this elastic estimation method is also unsuitable for modeling the relation between $V_L[111]$ and the alloy composition in $\text{In}_x\text{Ga}_{(1-x)}\text{As}$. Moreover, because the assumption of linear compositional dependence of the elastic constants failed, the results thus support that the elastic constants of $\text{In}_x\text{Ga}_{(1-x)}\text{As}$ would have a nonlinear relationship with the In contents. Since the linear-interpolation approximations with the sound velocity and the elastic constants both fail for modeling the $V_L[111]$ of $\text{In}_x\text{Ga}_{(1-x)}\text{As}$, a higher-order polynomial would be used to fit the nonlinear relation of the sound velocity. With a reference of the calculated sound velocity of InAs, the experimental results can be nicely described by a quadratic function of $V_L(x) = (458 \pm 35)x^2 - (1451 \pm 48)x + (5414 \pm 2)$, shown as the solid line in Fig. 4. This fitting curve agrees well with the expected values calculated from a previous measurement of the elastic constants of InGaAs whose In contents were 49% and 53%.¹⁰ It thus supports that the quadratic function can well describe the bowing characteristic of the discussed elastic property.

IV. CONCLUSION

We performed a picosecond ultrasonic experiment to generate acoustic pulses propagating in the [111] direction of $\text{In}_x\text{Ga}_{(1-x)}\text{As}$ and to directly examine its sound velocity dependence on the indium composition. The experimental results exhibit an obvious bowing in the sound velocity versus In composition x and can be well described using a quadratic function. This characteristic thus indicates the nonlinear compositional dependence of the elastic constants of $\text{In}_x\text{Ga}_{(1-x)}\text{As}$. Furthermore, our study experimentally demonstrates that the linear-interpolation approximation is inapplicable for estimating the sound velocity along the [111] direction of $\text{In}_x\text{Ga}_{(1-x)}\text{As}$.

ACKNOWLEDGMENTS

The authors would like to thank Y.-Y. Chen for inspiring scientific discussions. This work was sponsored by the National Science Council of Taiwan, R.O.C. under Grant No. 95-2120-M-002-013.

¹K.-H. Lin *et al.*, IEEE Trans. Ultrason. Ferroelectr. Freq. Control **52**, 1404 (2005).

²R. M. White and F. W. Voltmer, Appl. Phys. Lett. **7**, 314 (1965).

³K.-H. Lin, C.-T. Yu, Y.-C. Wen, and C.-K. Sun, Appl. Phys. Lett. **86**,

- 093110 (2005).
- ⁴C.-K. Sun, J.-C. Liang, and X.-Y. Yu, *Phys. Rev. Lett.* **84**, 179 (2000).
- ⁵C.-H. Chan, M.-C. Chen, H.-H. Lin, Y.-F. Chen, G.-J. Jan, and Y.-H. Chen, *Appl. Phys. Lett.* **72**, 1208 (1998).
- ⁶D. Royer and E. Dieulesaint, *Elastic Waves in Solids* (Springer, New York, 2000).
- ⁷See, for example, K. Brennan, *IEEE Trans. Electron Devices* **ED-33**, 1502 (1986).
- ⁸See, for example, S. Adachi, *J. Appl. Phys.* **58**, 1 (1985).
- ⁹N. Bouarissa, *Mater. Sci. Eng., B* **100**, 280 (2003).
- ¹⁰A. de Bernabe, C. Prieto, L. Gonzalez, Y. Gonzalez, and A. G. Every, *J. Phys.: Condens. Matter* **11**, L323 (1999).
- ¹¹M. Krieger, H. Sigg, N. Herres, K. Bachem, and K. Kohler, *Appl. Phys. Lett.* **66**, 682 (1995).
- ¹²C. Thomsen, H. T. Grahn, H. J. Maris, and J. Tauc, *Phys. Rev. B* **34**, 4129 (1986).
- ¹³T. C. Zhu, H. J. Maris, and J. Tauc, *Phys. Rev. B* **44**, 4281 (1991).
- ¹⁴H. T. Grahn, D. A. Young, H. J. Maris, J. Tauc, J. M. Hong, and T. P. Smith III, *Appl. Phys. Lett.* **53**, 2023 (1988).
- ¹⁵R. Liu *et al.*, *Phys. Rev. B* **72**, 195335 (2005).
- ¹⁶L.-W. Sung and H.-H. Lin, *Appl. Phys. Lett.* **83**, 1107 (2003).
- ¹⁷J. Zou, D. J. H. Cockayne, and B. F. Usher, *J. Appl. Phys.* **73**, 619 (1993).
- ¹⁸Y. Takano, K. Kobayashi, H. Iwahori, M. Umezawa, S. Shirakata, and S. Fuke, *Jpn. J. Appl. Phys., Part 1* **44**, 6403 (2005).
- ¹⁹T. Deguchi *et al.*, *J. Appl. Phys.* **86**, 1860 (1999).
- ²⁰D. D. Sell, H. C. Casey, Jr., and K. W. Wecht, *J. Appl. Phys.* **45**, 2650 (1974).
- ²¹R. E. Nahory, M. A. Pollack, and J. C. DeWinter, *J. Appl. Phys.* **46**, 775 (1975).
- ²²H.-N. Lin, R. J. Stoner, H. J. Maris, and J. Tauc, *J. Appl. Phys.* **69**, 3816 (1991).
- ²³G.-W. Chern, K.-H. Lin, and C.-K. Sun, *J. Appl. Phys.* **95**, 1114 (2004).
- ²⁴T. Takagi, *Jpn. J. Appl. Phys.* **17**, 1813 (1978).
- ²⁵R. I. Cottam and G. A. Saunders, *J. Phys. C* **6**, 2105 (1973).
- ²⁶S. L. Chuang, *Physics of Optoelectronic Devices* (Wiley, New York, 1995).
- ²⁷Y. J. Jung, B. H. Kim, H. J. Lee, and J. C. Woolley, *Phys. Rev. B* **26**, 3151 (1982).
- ²⁸D. L. Rode, *Phys. Rev. B* **3**, 3287 (1971).